Cerebral Cortex July 2014;24:1697–1707
doi:10.1093/cercor/bht023
Advance Access publication February 8, 2013

Network Connectivity and Individual Responses to Brain Stimulation in the Human Motor System

Lizbeth Cárdenas-Morales[1,2], Lukas J. Volz[1,2], Jochen Michely[1,2], Anne K. Rehme[1], Eva-Maria Pool[1], Charlotte Nettekoven[1], Simon B. Eickhoff[3,4], Gereon R. Fink[2,3] and Christian Grefkes[1,2]

[1]Neuromodulation and Neurorehabilitation, Max Planck Institute for Neurological Research, 50931 Cologne, Germany, [2]Department of Neurology, Cologne University Hospital, 50924 Cologne, Germany, [3]Institute of Neurosciences and Medicine (INM-1, INM-3), 52425 Juelich Research Centre, Juelich, Germany and [4]Institute for Clinical Neuroscience and Medical Psychology, Heinrich-Heine University, 40225 Düsseldorf, Germany

Address correspondence to Dr Christian Grefkes, Department of Neurology, Uniklinik Köln, Kerpener Straße 62, 50924 Köln, Germany. Email: christian.grefkes@uk-koeln.deL.C.-M. and L.J.V.contributed equally to the manuscript (shared first-authorship).

The mechanisms driving cortical plasticity in response to brain stimulation are still incompletely understood. We here explored whether neural activity and connectivity in the motor system relate to the magnitude of cortical plasticity induced by repetitive transcranial magnetic stimulation (rTMS). Twelve right-handed volunteers underwent functional magnetic resonance imaging during rest and while performing a simple hand motor task. Resting-state functional connectivity, task-induced activation, and task-related effective connectivity were assessed for a network of key motor areas. We then investigated the effects of intermittent theta-burst stimulation (iTBS) on motor-evoked potentials (MEP) for up to 25 min after stimulation over left primary motor cortex (M1) or parieto-occipital vertex (for control). ITBS-induced increases in MEP amplitudes correlated negatively with movement-related fMRI activity in left M1. Control iTBS had no effect on M1 excitability. Subjects with better response to M1-iTBS featured stronger preinterventional effective connectivity between left premotor areas and left M1. In contrast, resting-state connectivity did not predict iTBS aftereffects. Plasticity-related changes in M1 following brain stimulation seem to depend not only on local factors but also on interconnected brain regions. Predominantly activity-dependent properties of the cortical motor system are indicative of excitability changes following induction of cortical plasticity with rTMS.

Keywords: brain stimulation, neuromodulation, plasticity, repetitive TMS

Introduction

Fundamental processes of the brain like learning and acquisition of new motor skills depend on neuronal plasticity in a number of spatially distributed but interconnected brain regions. Methodological advances in neuroimaging and non-invasive brain stimulation—such as repetitive transcranial magnetic stimulation (rTMS)—have substantially furthered our knowledge on cortical plasticity and underlying mechanisms (for reviews, see, e.g., Censor and Cohen 2011; Dayan and Cohen 2011). Intermittent theta-burst stimulation (iTBS) is a specific type of rTMS that induces changes in cortical excitability beyond the stimulation period (Huang et al. 2005). When applied to the primary motor cortex (M1) iTBS increases the amplitudes of motor-evoked potentials (MEPs) subsequently induced by single-pulse TMS for up to 20 min (Huang et al. 2005; for a review, see Cárdenas-Morales et al. 2010).

It is widely assumed that long-term potentiation (LTP)- and long-term depression (LTD)-like processes induced by iTBS and other rTMS protocols (Huang et al. 2005, 2007), similar to what has been observed for in vitro stimulation of cortical synapses (Tsumoto 1992), may play an important role in the evolution of these stimulation aftereffects (Thickbroom 2007). There is, however, a considerable amount of interindividual variability in the response to iTBS (and also other rTMS protocols) which seems to depend on biological factors like age (Freitas et al. 2011) and genetic polymorphisms of the brain-derived neurotrophic factor (Kleim et al. 2006; Cheeran et al. 2008), but also on technical aspects such as the direction of current flow, the intensity of stimulation and the number of pulses applied (Talelli et al. 2007; Gentner et al. 2008; Gamboa et al. 2010). Recently, Hamada et al. (2012) showed that the activation of particular classes of interneurons by iTBS—as indicated by the recruitment of late indirect waves (I-waves)—accounts for parts of individual differences in stimulation aftereffects. Interestingly, these late I-waves were demonstrated to depend on influences exerted by premotor areas, and imply a crucial role of interneuron networks in human cortical plasticity (Shimazu et al. 2004; Lemon 2008). Therefore, the question arises whether remote areas might also influence the susceptibility to plasticity-inducing stimulation protocols like iTBS. Further support for this hypothesis derives from patient studies, linking decreased functional connectivity between premotor and primary motor cortex with higher susceptibility to rTMS in patients with dystonia (Quartarone et al. 2003; Koch et al. 2008; Huang et al. 2010). Moreover, rTMS does not only induce regional changes at the stimulation site (e.g., M1), but also in spatially remote parts of the brain (Bestmann et al. 2003, 2005; Esser et al. 2006; Suppa et al. 2008; Cárdenas-Morales et al. 2011). Consequently, it appears reasonable to assume that the physiological changes following an intervention also depend on how efficient the stimulated area (e.g., M1) is integrated into a given functional network, for example, the cortical motor system.

In the present study, we addressed the issue of the physiological mechanisms underlying motocortical plasticity from a system-level perspective using neuroimaging and models of connectivity (Friston 1994). We scanned a group of healthy subjects with functional magnetic resonance imaging (fMRI) during rest and while performing a simple hand motor task in order to test the hypothesis that the plasticity effects induced by iTBS on motocortical excitability are related to activity and connectivity of the motor system. Connectivity was tested prior to iTBS for a network consisting of key motor areas. Then, in 2 separate sessions, iTBS was either applied to the dominant (left) motor cortex or to a control stimulation site

over parieto-occipital cortex (Herwig et al. 2007; Herwig et al. 2010). MEPs were recorded for a period up to 25-min post-stimulation. We correlated changes in MEP amplitudes following iTBS of M1 (or control) to BOLD activity, functional resting-state, and dynamic causal modeling of effective connectivity within the cortical motor system. Previous studies using rTMS showed that the magnitude of intervention effects is related to M1 activity and its connectivity to premotor areas (Ameli et al. 2009; Grefkes et al. 2010; Wang et al. 2011). We, hence, hypothesized that individual patterns of neural activity in M1 and connectivity between M1 and other relevant motor areas indicate the susceptibility to a plasticity-enhancing stimulation protocol like iTBS applied over M1. Given the relationship between ventral premotor cortex (vPMC), late I-waves, and iTBS response (Shimazu et al. 2004; Lemon 2008; Hamada et al. 2012), we further reasoned that subjects showing strong connectivity of this area with M1 would show especially high magnitudes of changes in cortical excitability following stimulation with iTBS.

Materials and Methods

Subjects

Twelve healthy, right-handed volunteers (mean age: 39 ± 11 years; 5 females) were recruited. Exclusion criteria were a history of brain injury, neurologic, or psychiatric disease, the presence of any major medical illness, or an intake of any medication during the time of the study. All participants gave their written informed consent for the experiments, and were paid for participation. The project adhered to the Declaration of Helsinki and was approved by the Ethics Committee of the University of Cologne.

Experimental Design

The within-subject design comprised three different sessions performed on different days. In the first session, subjects underwent fMRI measurements during rest and during performance of a simple hand motor task. In the second and third sessions, either iTBS over the dominant (left) M1 or over parieto-occipital vertex (Pz, for control) was carried out in a randomized order with electrophysiological monitoring before and after intervention. The intersession interval was 2–3 days.

Functional MRI

All subjects first underwent resting-state fMRI followed by an fMRI while subjects performed an active motor task. MR images were acquired on a Siemens Trio 3.0 T scanner (Siemens Medical Solutions, Erlangen, Germany). Both paradigms were measured using a gradient echo-planar imaging (EPI) sequence with the following parameters: TR = 2200 ms, TE = 30 ms, FOV = 200 mm, 33 slices, voxel size: $3.1 \times 3.1 \times 3.1$ mm^3, 20% distance factor, flip angle = 90°, resting-state fMRI: 184 volumes, motor task fMRI: 283 volumes. The slices covered the whole brain extending from the vertex to lower parts of the cerebellum. In addition, high-resolution T_1-weighted structural images were acquired (TR = 2250 ms, TE = 3.93 ms, FOV = 256 mm, 176 sagittal slices, voxel size = $1.0 \times 1.0 \times 1.0$ mm^3).

For the resting-state paradigm, subjects were instructed to remain motionless and to fixate a red cross on a black screen during scanning. The fixation cross was presented on a shielded TFT screen at the rear end of the scanner, which was visible via a mirror mounted to the MR head coil. The resting-state session lasted about 7 min, as it has been shown that longer scanning times provide no significant improvement of signal-to-noise but promote fatigue of the subjects (Van Dijk et al. 2010). Preventing fatigue was also the reason for scanning the subjects with open eyes. The subjects were monitored by means of an MR compatible infrared camera attached to the end of the scanner.

The fMRI motor task consisted of visually cued hand movements with thumb abductions. Written instructions were displayed on the screen for 1 s indicating whether the left or the right hand had to be moved in the upcoming block of trials. Subjects were instructed to perform the movements for 14 s with maximum amplitude at a frequency of 1 Hz as indicated by a blinking circle until a black screen indicated to rest for the following 15 s. Subjects were trained outside and inside the scanner until they reached stable performance. Overall, the motor task used in the present study had only a few degrees of freedom, with a predefined movement amplitude and low movement frequency, so that subjects were readily able to perform the task with high stability after a few (2–3) practice trials. Note that the motor task activated the same muscles as used for TMS recordings (the left hand movements were necessary for localizing the motor areas of interest in the right hemisphere, which were also part of the connectivity model as described further below).

fMRI Preprocessing

FMRI data were analyzed using Statistical Parametric Mapping (SPM8; Wellcome Department of Imaging Neuroscience, London, UK, http://www.fil.ion.ucl.ac.uk). The first 4 volumes of each session ("dummy" images) were discarded from further analysis. The resting-state and the motor task EPI volumes were then realigned to the mean image of each time series and coregistered with the structural T_1-weighted image. For the group analyses, all images were spatially normalized to the standard template of the Montreal Neurological Institute (MNI, Canada) using the unified segmentation approach (Ashburner and Friston 2005). Finally, data were smoothed using an isotropic Gaussian kernel of 8-mm full-width at half-maximum.

For the resting-state data, variance that could be explained by known confounds was removed from the smoothed image time series. Confound regressors included the tissue-class-specific global signal intensities and their squared values, the 6 head motion parameters from realignment, their squared values as well as their first-order derivatives (Jakobs et al. 2012; Reetz et al. 2012). Data were band-pass filtered between 0.01 and 0.08 Hz.

Statistical Analysis: fMRI Motor Task Data

For the hand motor task, statistical analysis was performed in the framework of the general linear model (GLM). The experimental conditions were modeled using boxcar stimulus functions convolved with a canonical hemodynamic response function. The time series in each voxel were high-pass filtered at 1/128 Hz. The 6-head motion parameters, as assessed by the realignment algorithm, were treated as covariates to remove movement-related variance from the image time series. Simple main effects for each experimental condition were calculated for every subject by applying appropriate baseline contrasts. Voxels were identified as significant on the single-subject level if their t-values passed a height threshold of $T > 4.7$, corresponding to $P < 0.05$ (family-wise error [FWE] corrected for multiple comparisons at voxel level).

For fMRI group analyses, the parameter estimates of the experimental conditions were compared between subjects ($n = 12$) in a second-level GLM with the factor hand (levels "right" and "left"). For correlation analyses between movement-related BOLD activity and iTBS aftereffects (see below), the contrast images "right-hand movements versus rest" were entered into an SPM multiple regression analysis with the individual strength of the iTBS aftereffects on cortical excitability as covariate (see TMS Data Analysis section). As all TMS parameters were derived from the left motor hand area, we had a strong anatomical hypothesis with regard to the location of significant effects in left M1. We hence performed a small volume correction (SVC) using an 8-mm sphere centered at the hand knob formation (Yousry et al. 1997) of the precentral gyrus (MNI coordinates (x, y, z): −40, −20, 52).

Dynamic Causal Modeling

We used dynamic causal modeling (DCM; Friston et al. 2003) to estimate effective connectivity among key motor areas activated by the

fMRI motor task. DCM uses a bilinear model (Friston et al. 2003), where the changes in neuronal states over time are modeled as

$$\frac{dx}{dt} = \left(A + \sum_{j=1}^{m} u_j B^{(j)}\right)x + Cu$$

where x is the state vector, A represents the endogenous (intrinsic) connectivity, $B(j)$ represent the task-dependent modulations of the modeled region driven by the input function u (here: 0 or 1 due to the boxcar function of the block design employed in the fMRI experiment), and C represents the influence of direct inputs to the system. As becomes evident from this formulation, the endogenous connectivity (DCM-A matrix) is always present during the experiment and hence represents the task-independent component of interregional coupling. The task-dependent modulations represented in the B matrix, however, only contribute to the changes in neuronal states when the respective task is performed, that is, when the value input function is 1 (not, however, in the baseline condition). The bilinear model also indicates that endogenous connectivity should not be influenced or even driven by task-related activity. Rather, the latter will be independently modeled in addition to it. This, however, does not exclude that the coupling parameters correlate between DCM-A and DCM-B.

As DCMs are computed on the single-subject level, we extracted the BOLD time series (first eigenvariate) from 8 volumes of interest (VOIs) at subject-specific coordinates within 8-mm spheres around individually defined activation maxima in the normalized SPMs. The contrast "right hand movement versus rest" was used to localize the VOIs in the left hemisphere while the contrast "left hand movement versus rest" served to extract right hemispheric VOIs. All VOIs were defined by functional and anatomical criteria based on the individual activation maps superimposed on the corresponding structural T_1 volume using a-priori-defined anatomical constraints: M1 on the rostral wall of the central sulcus at the "hand knob" formation (Yousry et al. 1997), supplementary motor area (SMA) on the medial wall within the interhemispheric fissure between the paracentral lobule (posterior landmark) and the coronal plane running through the anterior commissure (Picard and Strick 2001), and vPMC close to the inferior precentral gyrus and pars opercularis (Rizzolatti et al. 2002). Also other areas constitute important nodes in the motor system. For example, the dorsal premotor cortex (dPMC) situated in superior precentral sulcus is a key region in movement planning, especially with respect to visually guided reaching movements (Rizzolatti and Luppino 2001; Prado et al. 2005). However, in DCM, the stability of model estimation limits the number of areas that can be included into a model (Penny et al. 2004; Stephan et al. 2009). As monkey studies showed that neurons in vPMC (areas F4/F5) are engaged in movements of the hands and fingers while neurons in dPMC rather code movements of the arm based on visual and somatosensory information (Dum and Strick 1992; Rizzolatti et al. 1998), we decided to include vPMC into our model as the fMRI task primarily addressed finger movements (which activated vPMC rather than dPMC, see Fig. 2). As subjects were requested to move their hands according to the frequency of the visual pacing cue, activity within the cortical motor system was assumed to be driven by the visual system. Strongest activity within the visual cortex was found at the occipital poles corresponding to the foveal representations in the primary visual cortex (V1), which was selected as sensory input region for DCM (Grefkes, Eickhoff et al. 2008). The individual coordinates for all VOIs are given in Table 1.

Connectivity Models

On the basis of published data on anatomical connectivity in macaque monkeys, we assumed endogenous connections between SMA and ipsilateral and contralateral M1 (Rouiller et al. 1994), between SMA and ipsilateral (Luppino et al. 1993) as well as contralateral vPMC (Boussaoud et al. 2005), between vPMC and both ipsi- and contralateral M1 (Rouiller et al. 1994), as well as homotopic transcallosal connections among M1–M1 (Rouiller et al. 1994), SMA–SMA (McGuire et al. 1991), and vPMC–vPMC (Boussaoud et al. 2005). Evidently, the condition-specific modulations of interregional coupling do not necessarily affect all possible anatomical connections. We, therefore, constructed 7 alternative models (see Supplementary Fig. 1) of connectivity representing biologically plausible hypotheses on interregional coupling. The models varied in complexity and numbers of connections ranging from sparsely (e.g., model 1) to fully connected models (e.g., model 7). We then used Bayesian model selection (Penny et al. 2004) to identify the model yielding the highest evidence given the data using a random effects approach (Stephan et al. 2009). Note that we did not employ model selection for the resting-state data as here coupling parameters (i.e., time-series correlations) are independently computed for each pair of connection (in contrast to DCM where the estimation of coupling parameters depends on model structure). The coupling parameters of the most likely generative model were tested for statistical significance by means of 1-sample t-tests for each experimental session (false discovery rate [FDR] corrected for multiple comparisons, $P < 0.05$) (Benjamini and Hochberg 1995). Correlation analyses between iTBS aftereffects and significant DCM coupling parameters were computed using Statistical Program of the Social Sciences (SPSS 19, Chicago, 2009), and finally FDR corrected for multiple comparisons.

Statistical Analysis: fMRI Resting-State Data

For the resting-state analysis, times series information (first eigenvariates) of the motor VOIs were extracted from the normalized EPIs at the very same coordinates as used in the DCM analysis. A seed-to-seed network analysis was computed by means of linear Pearson's correlations between resting-state time courses of all 6 motor VOIs ($P < 0.05$, FDR corrected). Correlation coefficients were converted to Fisher's Z-scores using the formula $Z = (1/2) \times \ln(1 + r)/(1 - r) = \text{artanh}(r)$ to yield approximately normally distributed data in the resting-state connectivity matrix. This network analysis was complemented by a seed-based whole-brain group analysis consisting of correlations

Table 1
Local maxima of fMRI BOLD-signal of each subject used as VOIs for DCM

Subject	V1_L	V1_R	SMA_L	SMA_R	vPMC_L	vPMC_R	M1_L	M1_R
1	−8 −96 −6	12 −96 −8	−6 −7 65	4 −7 56	−56 −4 28	54 14 26	−30 −26 62	32 −22 64
2	−4 −98 0	14 −98 −2	−8 −6 56	4 0 62	−46 2 42	52 10 32	−38 −24 60	34 −18 60
3	−10 −96 −20	18 −98 −10	−6 −8 70	10 0 60	−54 −6 42	58 −8 40	−32 −22 60	36 −20 60
4	−12 −92 −10	16 −98 −4	−6 −8 50	6 −6 66	−54 −16 38	56 −10 48	−34 −26 62	34 −18 58
5	−12 −96 −14	20 −96 −2	−4 −6 50	10 −2 58	−54 6 16	52 8 36	−36 −26 56	40 −26 52
6	−16 −94 −12	22 −92 −10	−6 −6 56	8 −6 60	−56 −2 40	58 4 38	−32 −26 56	32 −24 60
7	−4 −90 −10	22 −94 0	−4 −8 64	8 2 70	−42 −18 58	44 −10 60	−40 −24 58	40 −18 60
8	−10 −98 −10	18 −96 −2	−4 −8 54	6 −8 72	−58 4 34	56 0 46	−38 −22 48	34 −20 63
9	−10 −92 −14	14 −98 −10	−2 −6 60	6 2 56	−42 −8 36	46 4 40	−40 −18 58	36 −22 56
10	−10 −100 −8	12 −94 −8	−4 −4 56	8 2 58	−40 4 34	52 6 40	−34 −24 56	38 −24 54
11	−10 −96 −14	10 −94 −12	−4 0 54	4 4 62	−48 −6 48	56 4 44	−36 −24 58	32 −24 68
12	−10 −92 −14	14 −92 −10	−4 −4 58	8 4 54	−48 −6 46	54 −8 42	−36 −26 58	36 −24 56
Mean	−9 −95 −11	16 −95 −6	−5 −6 58	7 −1 61	−50 −4 38	53 1 41	−35 −20 57	35 −21 59
SD	3 3 5	4 2 4	2 2 6	2 4 5	6 8 10	4 8 8	3 3 3	2 2 4

between seed voxel time courses in stimulated left M1 and time courses of every other voxel in the brain (Eickhoff and Grefkes 2011; zu Eulenburg et al. 2012).

Transcranial Magnetic Stimulation

Single-pulse TMS was delivered using a monophasic Magstim 200^2 stimulator (Magstim Co., Whitland, Dyfed, UK). MEP amplitudes were measured from the right abductor pollicis brevis (APB) muscle using Ag/AgCl surface electrodes (Tyco Healthcare, Neustadt, Germany) with a belly-tendon montage. The EMG signal was amplified, filtered (0.5 Hz high-pass and 30–300 Hz band-pass) and digitized with a Powerlab 26T and LabChart software package version 5 (ADInstruments, Ltd., Dunedin, New Zealand). The position of the electrodes was photographed in a standard montage, and used as reference for the second iTBS session to minimize intersession variability.

The coil was positioned over the hand area of M1, tangentially to the scalp with the handle-pointing posterior. The "motor hotspot" over left M1 was defined as the location where MEPs could be evoked with highest amplitude and shortest latencies. The coil position was marked on the skull using a water-proof pen, and photographed as anatomical reference for the second iTBS session. The resting motor threshold (RMT) was defined as the lowest stimulus intensity that elicited at least five responses ≥50 μV within 10 consecutive single-pulses with the target muscle at rest (Rossini et al. 1994; Ziemann et al. 1996; Rothwell et al. 1999).

Theta Burst Stimulation

iTBS was delivered over the left M1 using a Magstim SuperRapid2 stimulator with a figure-of-eight coil (70-mm standard coil, Magstim Co., Whitland, Dyfed, UK). In line with other groups (Huang et al. 2005; Hamada et al. 2012) we did not use the SuperRapid2 stimulator for MEP acquisition as this stimulator can only induce biphasic waveforms of the TMS pulse. However, biphasic pulses induce a complex pattern of activation in the stimulated cortex exciting different neuronal populations during the different phases of the pulse, which results in less homogenous MEPs than those evoked by monophasic pulses (Terao and Ugawa 2002; Di Lazzaro et al. 2004). We, therefore, used the Magstim 200^2 stimulator to evoke MEPs with monophasic waveforms (Huang et al. 2005; Hamada et al. 2012). Note that the efficiency of iTBS in increasing cortical excitability was demonstrated not to dependent of the waveform (bi/monophasic) of the TMS pulse (Zafar et al. 2008).

iTBS consisted of 3 pulses delivered at a frequency of 50 Hz every 200 ms during 2 s (10 bursts) and repeated every 10 s for a total duration of 191 s (600 pulses) (Huang et al. 2005). We first determined the motor hotspot for the SuperRapid2-coil (posterior–anterior-oriented current) followed by the assessment of the RMT (RMTs were usually higher for the SuperRapid2 than for the Magstim 2002 stimulator). Then, iTBS was delivered at 70% RMT. Note that this is a slight modification with respect to the original iTBS protocol, which uses 80% active motor threshold (AMT, Huang et al. 2005). However, we assumed similar iTBS response as 70% RMT is usually in a similar range of absolute stimulator output intensities like 80% AMT (Chen et al. 1998; Gentner et al. 2008; Sarfeld et al. 2012). Control stimulation was delivered over the parieto-occipital vertex (Pz) using the same stimulator output intensity as for M1 stimulation. To reduce possible cortical stimulation effects in the control condition, the coil was angled at 45°, touching the skull not with the centre but with the rim opposite the handle. In this position, the coil–cortex distance is essentially larger such that the electromagnetic field, if at all reaching the cortex, is substantially weaker and far outside the target range (Herwig et al. 2007; Herwig et al. 2010).

Motor hotspots were defined for both stimulators and marked on the skull by means of a waterproof pen. MEP amplitudes evoked by monophasic single-pulse TMS (Magstim 200^2 stimulator) were evaluated before and after the delivery of iTBS.

Subjects were comfortably seated in an adjustable armchair with headrest. Baseline corticospinal excitability (in terms of MEPs) was assessed by measuring the amplitudes of 36 MEPs in the right APB muscle at rest as response to single-pulse TMS (posterior–anterior oriented current) applied with an intensity of 120% RMT at a frequency of 0.2 Hz. After iTBS, batches of MEPs to 12 single TMS pulses were recorded every 5 min for 25 min (120 RMT, 0.2 Hz) from the identical position as those evoked before stimulation (Huang et al. 2005).

TMS Data Analysis

In line with Huang et al. (2005), we analyzed iTBS aftereffects by means of a 2-way-repeated measures analysis of variance (ANOVA) of MEP amplitudes normalized to baseline assessments with the factors "intervention" (2 levels: M1-iTBS vs control-iTBS) and "time" (5 levels: "5 min," "10 min," "15 min," "20 min," "25 min"), followed up by *t*-tests comparing baseline and MEP amplitudes after different points in time testing for the temporal maximum of stimulation aftereffects.

For correlation analyses with neural activity and connectivity (BOLD signal, DCM, and resting-state parameters), we used 2 parameters as index for the strength of the iTBS aftereffects. 1) MEP amplitudes after 10 min (i.e., the point of time when strongest and most significant differences were observed between M1 and sham stimulation) and 2) the maximum MEP response (change in MEP amplitude relative to baseline) over the entire 25-min recording session. This means that we performed all correlation analyses twice, that is, for the 10-min post-iTBS values and for the maximum iTBS response over the whole session.

Statistical Correction for Multiple Comparisons

To obtain comparable statistical results, the same approach—FDR correction for multiple correlations—was used for all analyses performed in this study. This represents a trade-off between statistical sensitivity (given the large number of comparisons) and adjustment of *P* values required by multiple testing. However, for the main findings, we, in addition, also present Bonferroni corrected *P*-values in order to show the statistical robustness of the results.

Results

TMS and iTBS were well tolerated and no subject reported relevant side effects. Two participants with high motor thresholds reported mild headache after the experiment.

iTBS Aftereffects on Electrophysiological Parameters

Mean RMT was 44.5 ± 8.3% for iTBS and 43.0 ± 8.0% of maximal stimulator output for control stimulation. Baseline MEP amplitudes were not significantly different between M1-iTBS (0.69 ± 0.46 mV) and control-iTBS (0.80 ± 0.37 mV) (Student's *t*-test; $P = 0.259$). When testing for an intervention effect on normalized MEP amplitudes, a 2-way-repeated measures ANOVA showed a significant main effect for "intervention" ($F_{1,10} = 7.10$, $P = 0.022$) but not for "time" (Fig. 1). Although no significant interaction effect was evident ($P = 0.13$), which implied that iTBS over M1 induced a lasting increase in MEP amplitude, we used Student's *t*-tests to identify the point of time with maximal difference between sham and M1 stimulation (as in Huang et al. 2005). We found that M1-iTBS yielded the maximum effect, that is, largest and most significant differences in normalized MEP amplitudes between M1 and sham stimulation at 10 min following stimulation (5 min: $P = 0.047$, 10 min: $P = 0.022$, 15 min: $P = 0.059$). Hence, iTBS applied over M1 with 70% RMT significantly enhanced cortical excitability compared with both baseline and control stimulation (over Pz). No significant correlations were evident for iTBS aftereffects and electrophysiological baseline parameters (RMT: $r = -0.121$, $P = 0.708$; baseline MEP amplitudes: for sham- ($r = -0.162$, $P = 0.616$) and M1 stimulation ($r = -0.162$, $P = 0.614$).

fMRI BOLD Data and iTBS Aftereffects

All subjects were readily able to perform the task with the requested frequency and movement amplitude after a few seconds of training due to the relative simplicity of the motor task. Training was performed for the first 3 blocks of trials in order to control for habituation effects (scanner environment, position of the hands, etc.).

The fMRI group analysis showed that compared with no-movement (baseline), right-hand movements were associated with enhanced BOLD activity in a left-lateralized network comprising left M1, SMA, bilateral vPMC, bilateral primary, and higher visual areas (V1–V5), as well as subcortical regions like left thalamus, left putamen, and right anterior cerebellum (see Fig. 2*A*; $P < 0.05$, FWE corrected at the voxel level). Movements of the left hand yielded a similar, yet mirror-reversed network of activity.

In order to test whether the fMRI BOLD signal during movements of the right hand was related to the iTBS aftereffect on MEP amplitudes, we performed an SPM multiple regression analysis of the respective individual contrast images and the relative increase of MEP amplitudes (percentage compared with baseline) after 10 min (referring to the moment of strongest iTBS aftereffects upon M1 stimulation, see above). This analysis showed a negative correlation between iTBS aftereffects and the BOLD signal in a cluster of voxels at the motor hand knob (see Fig. 2*B*; local maximum at MNI coordinates (x, y, z): −40, −20, 52; $T = 2.84$, $P = 0.048$; small volume corrected on the voxel level): Subjects showing stronger M1-iTBS aftereffects were those with less preinterventional task-related neural activity in the stimulated area. Furthermore, when plotting this cluster of voxels correlating with iTBS aftereffects together with the peak activation cluster for movements of the respective hand, we observed that the local activation maxima did not overlap but lay adjacent to each other (see Supplementary Fig. 3). This means that those subjects who had more extended activation clusters around the group local maximum were those with less response to iTBS.

When correlating the imaging data with the maximum iTBS aftereffect over the 25-min recording session, we only found a trend toward significance in the same M1 cluster ($P < 0.1$). No further correlations between neural activation within other motor regions than M1- and iTBS-effects were evident. The equivalent correlation with the MEP data from the control-iTBS session did not yield any significant result.

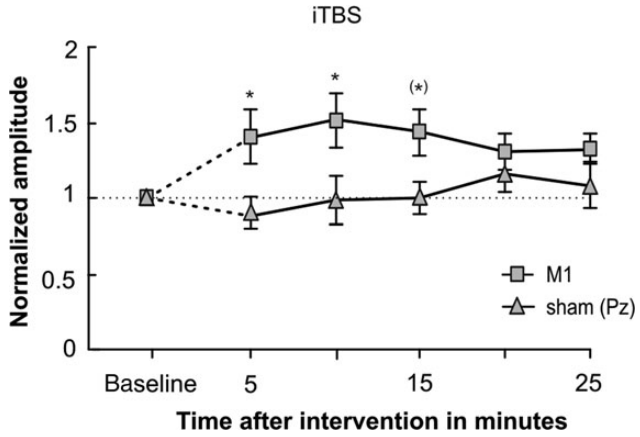

Figure 1. Changes in MEP amplitude following real- (squares) and sham-iTBS (triangles), normalized to prestimulation MEP amplitudes. Asterisk indicates significant aftereffect following real-iTBS compared with sham; $P < 0.05$; Student's t-test.

Resting-State Connectivity and iTBS Aftereffects

The group analysis showed that during the resting-state, interregional coupling among the motor VOIs was predominantly significant for interhemispheric connections, that is, between SMA-SMA, vPMC-vPMC, M1-M1; left SMA-right vPMC; right SMA-left vPMC and left SMA-right M1 ($P < 0.05$, FDR corrected). The analysis further revealed significant intrahemispheric resting-state coupling between SMA and vPMC in both hemispheres, as well as a significant connection between left SMA-left M1 (see Fig. 3*B*). More importantly, there was no significant correlation between any of the resting-state parameters and iTBS aftereffects ($P > 0.1$, for all comparisons). Likewise, correlations between individual left M1 seed voxel maps and iTBS aftereffect sizes did not show significant effects. Hence, in our sample of subjects, we did not find a significant relationship between resting-state coupling of M1 and iTBS aftereffects.

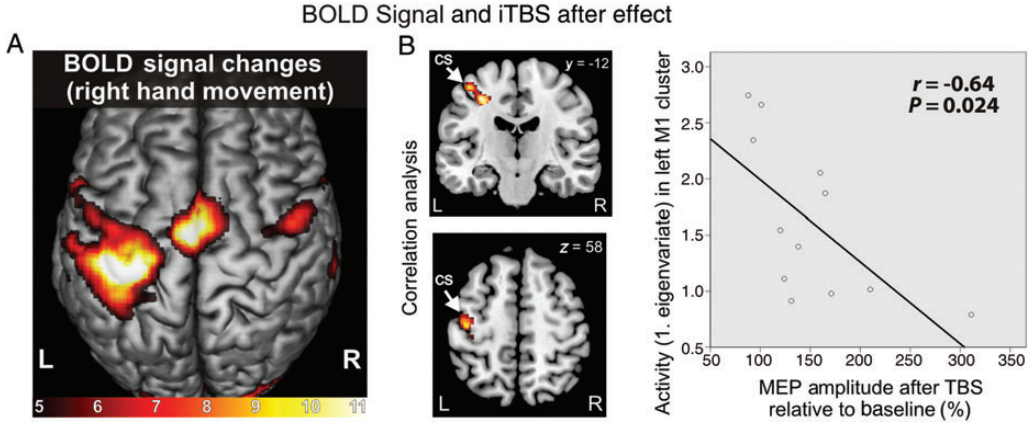

Figure 2. (*A*) BOLD activation changes during the movement of the right hand ($P < 0.05$; FWE corrected at voxel level; color bar represents t-values). Activation clusters were surface-rendered onto canonical brain. (*B*) SPM regression analysis: cluster of neural activation at the hand knob area negatively correlated with iTBS aftereffects (changes in MEP amplitude 10-min post-stimulation; $r = -0.64$, $P < 0.05$, SVC corrected on the voxel level). CS, central sulcus; L, left; R, right.

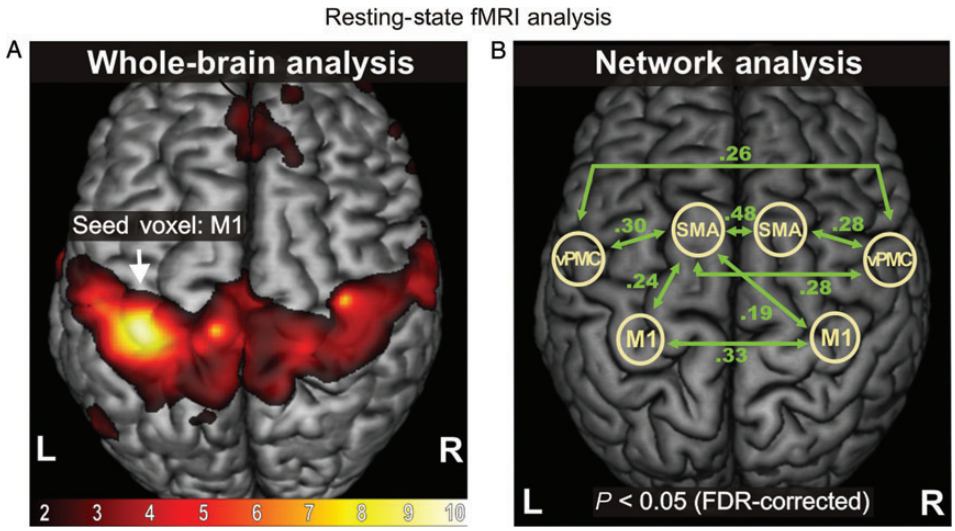

Figure 3. Resting-state fMRI analysis. (*A*) Seed-based whole-brain group analysis (seed region: left M1; MNI coordinates −36 −24 58, that is, the local maximum of the group analysis in Fig. 2*A*). Correlated fMRI time courses were not only found in the vicinity of the seed voxel, but also in homotopic regions in the contralateral hemisphere (voxel threshold: $P < 0.05$; color bar represents *t*-values). However, these correlations did not predict the iTBS aftereffects. (*B*) Network analysis testing for correlated resting-state activity in key regions of the motor system. Coordinates were derived from the motor task data of each individual subjects. We found strongly correlated (linear Pearson's correlations; $P < 0.05$, FDR corrected) BOLD times courses especially for interhemispheric connections as well as for intrahemispheric coupling between left SMA and M1, as well as left SMA and right M1 (correlation coefficients given as Fisher's *z*-scores). M1, primary motor cortex; SMA, supplementary motor area; vPMC, ventral premotor cortex.

DCM Connectivity and iTBS Aftereffects

We tested 7 alternative models of interregional connectivity (see Supplementary Fig. 1). These models varied in complexity and numbers of connections ranging from sparsely (e.g., model 1) to fully connected models (e.g., model 7). The experimental input (C matrix) was set to bilateral V1 for all models, as visual cues were used to trigger the movement frequency during the fMRI motor task. We assumed connections between bilateral V1 and all nodes of our network. It is essential to note that coupling parameters obtained from DCM refer to functional interactions, but do not necessarily reflect direct axonal connections. For example, the relay of visual information toward the premotor regions, e.g., via parietal regions that were not explicitly modeled in the DCM should be implicitly reflected in the derived rate constants of our model for effective connectivity within the cortical motor system. The model selection procedure identified model 7 (see Supplementary Fig. 1) with fully connected VOIs as the most likely generative model given the data.

Endogenous Coupling

Endogenous coupling (DCM-A matrix) refers to the coupling of areas independent of the effect of condition, that is, whether subjects moved the left or right hand. Note that this is not equivalent to an analysis of the resting-state as the whole times series information including the movement conditions are used to estimate endogenous connectivity. Therefore, endogenous coupling represents the constant component of connectivity in the activated motor system.

Overall, endogenous connectivity between the motor areas of interest was symmetrically organized across hemispheres ($P < 0.05$, FDR corrected for multiple comparisons). Endogenous coupling within the left or right hemisphere was positive for the interaction between the SMA, vPMC, and M1 with strongest effects for connections targeting M1. A negative coupling was found for interhemispheric connections among both M1, indicating an inhibitory connection among bilateral M1 (see Supplementary Fig. 2).

There were significant ($P < 0.05$, FDR corrected) positive correlations between iTBS aftereffects and endogenous coupling parameters from left SMA to left vPMC ($r = 0.81$, $P = 0.021$), from left vPMC to left M1 ($r = 0.78$, $P = 0.028$), and from left M1 to left vPMC ($r = 0.74$, $P = 0.048$). After Bonferroni correction, the connection from left SMA to left vPMC remained significant ($r = 0.81$, $P = 0.043$), while the coupling from left vPMC to left M1 showed a trend of significance ($r = 0.78$, $P = 0.083$). Hence, in contrast to the resting-state data, the iTBS-effect on excitability of left M1 was predicted by a stronger preinterventional, endogenous coupling of premotor areas with left M1. There were no significant correlations between endogenous coupling parameters and control-iTBS aftereffects.

Hand Movement-Specific Coupling

The modulation of interregional coupling induced by moving the right hand featured increases in the promoting influences of left vPMC and left SMA with left M1, but also inhibition of right M1 (see Fig. 4; $P < 0.05$, FDR corrected). Movements of the left hand were associated with a similar yet mirror-reversed modulation of coupling. The DCM-A and DCM-B matrices yielded a weak but significant correlation ($r = 0.473$, $P = 0.008$). This means that subjects with higher intrinsic/endogenous coupling parameters also showed a stronger modulation of these connections during movements of the right hand.

For correlations with iTBS aftereffects, we only considered coupling parameters estimated for data recorded during movements of the right hand, as MEPs were recorded from the right APB muscle. Here, we found significant correlations (FDR corrected for multiple comparisons) for couplings from left SMA to left vPMC ($r = 0.85$, $P = 0.004$), from left vPMC to left SMA ($r = 0.79$, $P = 0.010$), from left vPMC to left M1

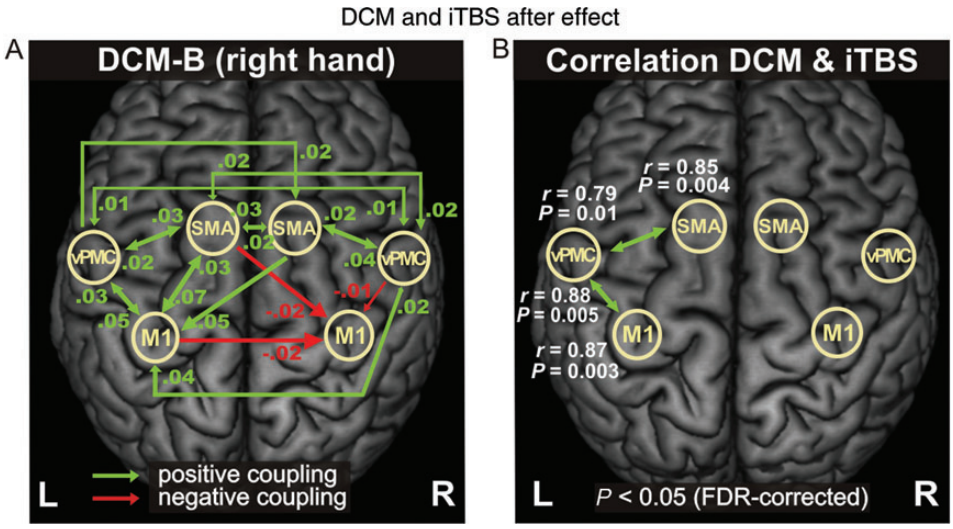

Figure 4. (*A*) Effective connectivity during movements of the right hand as estimated by dynamic causal modeling (DCM-B; green arrows represent positive coupling, red arrows indicate negative coupling). Strongest coupling estimates were found for interactions targeting left M1, while neural activity in right M1 was inhibited by both intra- and interhemispheric interactions ($P < 0.05$, FDR corrected for multiple comparisons) (*B*) Significant correlations of DCM coupling parameters with iTBS aftereffects ($P < 0.05$, FDR corrected). Here, high preinterventional coupling estimates between left vPMC and left SMA as well as between left vPMC and M1 predicted stronger iTBS aftereffects after 10 min. Note that VOIs were identical to those used for the resting-state analysis (Fig. 3). Abbreviations as in Figure 3.

($r = 0.87$, $P = 0.003$), and from left M1 to left vPMC ($r = 0.88$, $P = 0.005$). All of these connections remained significant after Bonferroni correction for multiple comparisons (SMA-vPMC: $P = 0.013$; vPMC-M1: $P = 0.006$; M1-vPMC: $P = 0.005$), except the coupling from left vPMC to left SMA ($P = 0.072$), which showed a statistical trend. That is, greater M1-iTBS aftereffects most likely occurred in subjects with stronger excitatory couplings between left SMA and vPMC as well as between left vPMC and M1. Of note, all significant effects were found for connections within the stimulated hemisphere although also coupling parameters of the nonstimulated (i.e., right) hemisphere were considered in the analysis. The same connections also significantly correlated when using the maximum effect across the 25 recording sessions as covariate ($P < 0.05$, for all comparisons). Control-iTBS aftereffects did not yield any significant correlations.

Discussion

ITBS applied over left M1 was well tolerated and resulted in significant enhancement of cortical excitability for up to 10 min with a strong statistical trend for 15 min. Two prestimulation settings correlated with individual iTBS susceptibility as indexed by higher poststimulation MEPs: 1) a relatively focal and low level of movement induced BOLD-activity in the left stimulated M1 and 2) strong intrahemispheric excitatory couplings between left SMA and left vPMC, and from left vPMC driving the stimulated (left) M1. In contrast, individual iTBS aftereffects were not predicted by functional connectivity of these areas during resting-state. Our data hence strongly suggest that predominantly activity-dependent properties of the cortical motor system, especially among M1, vPMC, and SMA, are indicative of excitability changes following induction of cortical plasticity with iTBS.

Modulating Cortical Excitability with iTBS

The cellular and neurophysiological mechanisms underlying iTBS-effects to date remain poorly understood (Thickbroom 2007; Cárdenas-Morales et al. 2010). One hypothesis is that rTMS protocols like iTBS induce synaptic plasticity changes, comparable with LTP—like effects, similar to what has been observed for the stimulation of preparations of synaptic connections in vitro (Tsumoto 1992). Neuropharmacological studies showed that the response to iTBS is—at least partially—dependent on NMDA-receptor activity (Huang et al. 2007; Teo et al. 2007), resembling LTP-like effects observed in animal studies (Hrabetova and Sacktor 1997). Another mechanism possibly involved in the evolution of iTBS aftereffects lies in the alteration of the cortical inhibitory system, as suggested by human electrophysiological (Di Lazzaro et al. 2008) and animal studies (Benali et al. 2011; Funke and Benali 2011). However, the individual responses to iTBS have been shown to be relatively variable (Ridding and Ziemann 2010) which is relevant when using iTBS to manipulate cortical excitability. Hamada et al. (2012) found that about 50% of variability regarding the individual susceptibility to iTBS could be explained by which forms of I-waves (early/late; depending on different MEP latencies upon different coil orientations) can be recruited in a given subject. These I-waves evolve depending on which types of interneurons are affected by the stimulation (Hamada et al. 2012). Such an interpretation is supported by recent findings in animal models which showed that iTBS interferes with the activity of distinct subgroups of inhibitory interneurons in the cortex of the rat (Funke and Benali 2011) as indicated by changes in the expression of activity-dependent proteins like the calcium-binding proteins Parvalbumin and Calbindin.

Neural Activation and iTBS Aftereffects

We found that both fMRI activities at the stimulation site as well as strong connectivity within the motor network of the stimulated hemisphere are indicative of a better response to iTBS. Although a simple fMRI motor task was used in this study subtle variation in task performance between subjects (e.g., differences in force, timing, or velocity) might have

increased the experimental variance (i.e., "noise"). Therefore, it might well be that also activity and connectivity of other areas are related to plasticity-inducing effects, albeit to a weaker degree than the significant findings in the present study (representing the most robust effects). However, as the main focus of the present study was to investigate the role of connectivity in stimulation aftereffects, we rather preferred a simple motor task with robust BOLD activation patterns, as for DCM a reliable definition of the regions of interest is mandatory in the individual SPMs of each and every subject.

ITBS applied over left M1 compared with control stimulation was demonstrated to decrease BOLD activity in M1 during a right hand choice-reaction task (button-press task upon visual cue) (Cárdenas-Morales et al. 2011). These findings probably reflect increased efficacy of neural signal transmission resulting in less neural activity required to accomplish the motor task. In line with this assumption, we found a negative correlation between changes of MEP amplitudes following iTBS and larger clusters of movement-related M1 stimulation prior to stimulation. Our data hence suggest that subjects with more focused M1 BOLD activity (possibly reflecting that less neural resources were needed to perform the task) were more responsive to iTBS. In healthy subjects, extended motor system activity is typically observed during learning of a new motor skill, which focuses during consolidation (Toni et al. 1998; Floyer-Lea and Matthews 2004; Park et al. 2010). In patient populations with motor impairments, we usually observe more extended, that is, less focal activity in motor areas, which focuses during the process of motor recovery (Chollet et al. 1991; Ward et al. 2003; Eickhoff et al. 2008; Grefkes, Nowak et al. 2008). Hence, more extended activity and less premotor–M1 connectivity are indicative for lower levels of motor performance and/or more effort to perform a given motor task. Accordingly, a more focal pattern of task-induced BOLD activity in M1 reflects a more efficient cortical motor network, which might have more capacity to respond to a plasticity-enhancing intervention. We thus speculate that subjects who showed a strong response to iTBS had "a more efficient" intrinsic motor network architecture with less need to recruit larger parts of M1 when moving the hand (i.e., more focused M1 cluster, cf., Supplementary Fig. 3) which in turn might have enabled them to recruit these "inactive" portions of M1 cortex following stimulation.

Connectivity and iTBS Aftereffects

Focally applied interventions like rTMS do not only have effects on the stimulated region, but may also affect activity in interconnected regions remote from the stimulation site (Bestmann et al. 2003, 2005; Suppa et al. 2008; Cárdenas-Morales et al. 2011). Likewise, the response to rTMS applied over M1 can be modulated by prior stimulation (priming) of remote areas as demonstrated for contralateral M1 (Ragert et al. 2009) and ipsilateral SMA (Hamada et al. 2009). Our data show that certain aspects of the connectivity state of the stimulated brain region are related to the individual amount of change in cortical excitability following iTBS and therefore possibly contribute to the evolution of cortical plasticity within the cortical motor network.

In the current study, we found no significant correlations between resting-state connectivity and iTBS-effects neither for seed-to-seed voxel analyses nor for M1-functional connectivity maps. This finding suggests that resting-state properties of the motor system have (if at all) only little predictive value for iTBS aftereffects. One potential caveat to this null result is that fMRI and TMS measurements were not assessed in the same session, and hence connectivity might have changed from the time of the resting-state measurements to the actual stimulation. Evidently, such short-term changes would not be reflected in the current analysis. However, earlier studies found a moderate to high test–retest reliability of functional resting-state connectivity (Shehzad et al. 2009; Van Dijk et al. 2010), making this scenario less likely. DCM applied to fMRI data has also been shown to be highly reliable between sessions (Schuyler et al. 2010). Moreover, the fact that fMRI activity and DCM connectivity pattern recorded at the same session in which the resting-state data were acquired were highly correlated with iTBS aftereffects further implies a relative stability of the data. Furthermore, other groups found evidence that resting-state assessments of brain activity are only poorly correlated with TBS susceptibility, for example, when compared with electroencephalography (EEG) recordings (McAllister et al. 2011). These data well match our resting-state fMRI results which also were nonpredictive for iTBS aftereffects. Our finding that stronger active-state connectivity between motor areas indicated a better response to iTBS aftereffects resembles data reported for the auditory system where stronger DCM connectivity of the primary auditory cortex predicted a better response to rTMS (Andoh and Zatorre 2011). Interestingly, in the present study also endogenous coupling among the motor areas (DCM-A) in the stimulated hemisphere was related to iTBS aftereffects albeit not as strong as observed for the additional effect induced by movements of the right hand. While it may seem puzzling at first that endogenous coupling in DCM is related to iTBS aftereffects whereas the "endogenous" resting-state connectivity is not, this apparent discrepancy is readily resolved when considering that, in these 2 cases, the term "endogenous" has vastly different meanings. In DCM, endogenous connectivity represents the constant part of connectivity in the activated motor system, which also includes the entire task set and—in contrast to resting-state scans—is specific to a particular fMRI experiment (Friston et al. 2003). Therefore, a possible interpretation is that the biological factors facilitating the coupling of motors areas in the activated motor system might also enable a higher susceptibility to plasticity-enhancing interventions like iTBS. For example, lesions to gray or white matter were demonstrated to reduce endogenous coupling between premotor areas and M1 concurrent to reduced motor performance in stroke patients (Grefkes, Nowak et al. 2008; Grefkes et al. 2010; Rehme et al. 2011; Wang et al. 2011). Both the lateral premotor cortex and the SMA region have dense axonal connections with M1, and both areas are known to be critical for motor planning and control (Jenkins et al. 2000; Schubotz and von Cramon 2003; Hoshi and Tanji 2004, 2007). Therefore, one explanation for our finding is that higher coupling of M1 with premotor areas reflects stronger activity-dependent synaptic transmission, which might impact on the susceptibility of neuronal excitability to iTBS.

Premotor Connectivity and iTBS Aftereffects

A more specific interpretation is possible for the significant correlation between the excitatory coupling from left vPMC to

left M1 and iTBS aftereffects: Hamada et al. (2012) found that individual aftereffects of iTBS might depend on individual differences in the recruitment of cortical neurons simulated with TMS. Subjects in whom late I-waves (estimated by latency differences of MEPs computed for different coil orientations) were recruited showed high susceptibility to iTBS. Late I-waves are a part of the MEP generated by stimulation of M1, possibly reflecting the input of complex oligosynaptic circuits to corticospinal neurons located in M1 (Hamada et al. 2012). These late I-waves have been shown to be enhanced following iTBS (Di Lazzaro et al. 2008). Electrophysiological studies in macaques demonstrated that late I-waves are strongly influenced by input from neurons located in vPMC (Shimazu et al. 2004; Lemon 2008). This relationship fits well with our data, which showed that effective connectivity between vPMC and M1 was a strong predictor for iTBS aftereffects. However, whether or not I-waves are related to connectivity parameters assessed with fMRI remains to be explored in future studies.

Furthermore, an alternative line of interpretation of our findings is that not only vPMC and M1, but the entire motor system is engaged in the aftereffects following M1 stimulation. Given the finding that the iTBS-effects correlated with connectivity among M1, vPMC, and SMA not only for the feedforward, but also for the feedback directions, we hypothesize that this connection pattern represents the network's ability to successfully propagate activity between cortical motor regions. TMS experiments performed during fMRI acquisition showed that M1 stimulation does not only induce BOLD activity in the stimulated region but also in interconnected motor regions like SMA and premotor cortex (Bestmann et al. 2003). This fits perfectly with our findings that plasticity-enhancing stimulation effects were associated with the connectivity strength among these regions. Therefore, an interesting (but speculative) interpretation of these relationships is that the whole system including the SMA and premotor cortex rather than a single area only might contribute to intervention effects. Support for this hypothesis is found in a study published by Ameli et al. (2009) who could show that stroke patients with lesions affecting the premotor cortex but sparing the M1 hand knob region are less responsive to excitability enhancing 10-Hz rTMS. Such effects might, for example, result from disrupted connectivity of the stimulation site, which would nicely fit the interpretation of the present data. Hence, the individual ability to strongly interconnect important cortical motor regions might underlie the induction of cortical plasticity within the cortical motor network (as indicated by the correlation with the individual changes in cortical excitability following iTBS).

Esser et al. (2006) demonstrated changes in premotor cortex activity after iTBS applied to M1 using high-density EEG. In the present study, we did not assess fMRI after iTBS as the primary objective of the study was to investigate the relationship between connectivity and variability in motor cortex plasticity induced by noninvasive brain stimulation. Other studies have already demonstrated that rTMS may interfere with connectivity not only at the stimulation site, but also between remote areas (Grefkes et al. 2010). However, the effects of iTBS on motor system connectivity remains to be elucidated in future studies.

Conclusions

iTBS aftereffects on M1 excitability are robustly predicted by a low level of BOLD activity at the stimulation site as well as strong effective connectivity among premotor areas, and a strong excitatory coupling from vPMC to M1. In contrast, there was no association with connectivity measured at rest. Importantly, our data confirm that cortical plasticity as induced by iTBS not only depends on local features of the stimulated cortex but is also influenced by interactions with remote cortical areas. Here, our data suggest that especially the ventral premotor cortex plays a crucial role in modulating iTBS responses in M1. Furthermore, the task-dependent interplay of M1, vPMC, and SMA seems to be involved in changes in cortical excitability and therefore cortical plasticity within the human motor network.

Supplementary Material

Supplementary material can be found at: http://www.cercor.oxfordjournals.org/.

Funding

C.G. was supported by a grant provided by the German Research Foundation (Deutsche Forschungsgemeinschaft, GR 3285/2-1).

Notes

We thank Dr. Marc Tittgemeyer and the MR staff for technical support. We also thank Dr. Masashi Hamada from the Sobell Department of Motor Neuroscience for valuable discussions. *Conflict of Interest*: None declared.

References

Ameli M, Grefkes C, Kemper F, Riegg FP, Rehme AK, Karbe H, Fink GR, Nowak DA. 2009. Differential effects of high-frequency repetitive transcranial magnetic stimulation over ipsilesional primary motor cortex in cortical and subcortical middle cerebral artery stroke. Ann Neurol. 66:298–309.

Andoh J, Zatorre RJ. 2011. Interhemispheric connectivity influences the degree of modulation of TMS-induced effects during auditory processing. Front Psychol. 2:161.

Ashburner J, Friston KJ. 2005. Unified segmentation. Neuroimage. 26:839–851.

Benali A, Trippe J, Weiler E, Mix A, Petrasch-Parwez E, Girzalsky W, Eysel UT, Erdmann R, Funke K. 2011. Theta-burst transcranial magnetic stimulation alters cortical inhibition. J Neurosci. 31:1193–1203.

Benjamini Y, Hochberg Y. 1995. Controlling the false discovery rate: a practical and powerful approach to multiple testing. J R Stat Soc Ser B (Methodological). 57:289–300.

Bestmann S, Baudewig J, Siebner HR, Rothwell JC, Frahm J. 2005. BOLD MRI responses to repetitive TMS over human dorsal premotor cortex. Neuroimage. 28:22–29.

Bestmann S, Baudewig J, Siebner HR, Rothwell JC, Frahm J. 2003. Subthreshold high-frequency TMS of human primary motor cortex modulates interconnected frontal motor areas as detected by interleaved fMRI-TMS. Neuroimage. 20:1685–1696.

Boussaoud D, Tanne-Gariepy J, Wannier T, Rouiller EM. 2005. Callosal connections of dorsal versus ventral premotor areas in the macaque monkey: a multiple retrograde tracing study. BMC Neurosci. 6:67.

Cárdenas-Morales L, Gron G, Kammer T. 2011. Exploring the aftereffects of theta burst magnetic stimulation on the human motor

cortex: a functional imaging study. Hum Brain Mapp. 32: 1948–1960.
Cárdenas-Morales L, Nowak DA, Kammer T, Wolf RC, Schonfeldt-Lecuona C. 2010. Mechanisms and applications of theta-burst rTMS on the human motor cortex. Brain Topogr. 22:294–306.
Censor N, Cohen LG. 2011. Using repetitive transcranial magnetic stimulation to study the underlying neural mechanisms of human motor learning and memory. J Physiol. 589:21–28.
Cheeran B, Talelli P, Mori F, Koch G, Suppa A, Edwards M, Houlden H, Bhatia K, Greenwood R, Rothwell JC. 2008. A common polymorphism in the brain-derived neurotrophic factor gene (BDNF) modulates human cortical plasticity and the response to rTMS. J Physiol. 586:5717–5725.
Chen R, Tam A, Butefisch C, Corwell B, Ziemann U, Rothwell JC, Cohen LG. 1998. Intracortical inhibition and facilitation in different representations of the human motor cortex. J Neurophysiol. 80:2870–2881.
Chollet F, DiPiero V, Wise RJ, Brooks DJ, Dolan RJ, Frackowiak RS. 1991. The functional anatomy of motor recovery after stroke in humans: a study with positron emission tomography. Ann Neurol. 29:63–71.
Dayan E, Cohen LG. 2011. Neuroplasticity subserving motor skill learning. Neuron. 72:443–454.
Di Lazzaro V, Oliviero A, Pilato F, Saturno E, Dileone M, Mazzone P, Insola A, Tonali PA, Rothwell JC. 2004. The physiological basis of transcranial motor cortex stimulation in conscious humans. Clin Neurophysiol. 115:255–266.
Di Lazzaro V, Pilato F, Dileone M, Profice P, Oliviero A, Mazzone P, Insola A, Ranieri F, Meglio M, Tonali PA et al. 2008. The physiological basis of the effects of intermittent theta burst stimulation of the human motor cortex. J Physiol. 586:3871–3879.
Dum RP, Strick PL. 1992. Medial wall motor areas and skeletomotor control. Curr Opin Neurobiol. 2:836–839.
Eickhoff SB, Dafotakis M, Grefkes C, Shah NJ, Zilles K, Piza-Katzer H. 2008. Central adaptation following heterotopic hand replantation probed by fMRI and effective connectivity analysis. Exp Neurol. 212:132–144.
Eickhoff SB, Grefkes C. 2011. Approaches for the integrated analysis of structure, function and connectivity of the human brain. Clin EEG Neurosci. 42:107–121.
Esser SK, Huber R, Massimini M, Peterson MJ, Ferrarelli F, Tononi G. 2006. A direct demonstration of cortical LTP in humans: a combined TMS/EEG study. Brain Res Bull. 69:86–94.
Floyer-Lea A, Matthews PM. 2004. Changing brain networks for visuomotor control with increased movement automaticity. J Neurophysiol. 92:2405–2412.
Freitas C, Perez J, Knobel M, Tormos JM, Oberman L, Eldaief M, Bashir S, Vernet M, Pena-Gomez C, Pascual-Leone A. 2011. Changes in cortical plasticity across the lifespan. Front Aging Neurosci. 3:5.
Friston KJ. 1994. Functional and effective connectivity in neuroimaging: a synthesis. Hum Brain Mapp. 2:56–78.
Friston KJ, Harrison L, Penny W. 2003. Dynamic causal modelling. Neuroimage. 19:1273–1302.
Funke K, Benali A. 2011. Modulation of cortical inhibition by rTMS-findings obtained from animal models. J Physiol. 589: 4423–4435.
Gamboa OL, Antal A, Moliadze V, Paulus W. 2010. Simply longer is not better: reversal of theta burst after-effect with prolonged stimulation. Exp Brain Res. 204:181–187.
Gentner R, Wankerl K, Reinsberger C, Zeller D, Classen J. 2008. Depression of human corticospinal excitability induced by magnetic theta-burst stimulation: evidence of rapid polarity-reversing metaplasticity. Cereb Cortex. 18:2046–2053.
Grefkes C, Eickhoff SB, Nowak DA, Dafotakis M, Fink GR. 2008. Dynamic intra- and interhemispheric interactions during unilateral and bilateral hand movements assessed with fMRI and DCM. Neuroimage. 41:1382–1394.
Grefkes C, Nowak DA, Eickhoff SB, Dafotakis M, Kust J, Karbe H, Fink GR. 2008. Cortical connectivity after subcortical stroke assessed with functional magnetic resonance imaging. Ann Neurol. 63:236–246.
Grefkes C, Nowak DA, Wang LE, Dafotakis M, Eickhoff SB, Fink GR. 2010. Modulating cortical connectivity in stroke patients by rTMS assessed with fMRI and dynamic causal modeling. Neuroimage. 50:233–242.
Hamada M, Hanajima R, Terao Y, Okabe S, Nakatani-Enomoto S, Furubayashi T, Matsumoto H, Shirota Y, Ohminami S, Ugawa Y. 2009. Primary motor cortical metaplasticity induced by priming over the supplementary motor area. J Physiol. 587:4845–4862.
Hamada M, Murase N, Hasan A, Balaratnam M, Rothwell JC. 2013. The Role of Interneuron Networks in Driving Human Motor Cortical Plasticity. Cereb Cortex. 23:1593–1605.
Herwig U, Cardenas-Morales L, Connemann BJ, Kammer T, Schonfeldt-Lecuona C. 2010. Sham or real-post hoc estimation of stimulation condition in a randomized transcranial magnetic stimulation trial. Neurosci Lett. 471:30–33.
Herwig U, Fallgatter AJ, Hoppner J, Eschweiler GW, Kron M, Hajak G, Padberg F, Naderi-Heiden A, Abler B, Eichhammer P et al. 2007. Antidepressant effects of augmentative transcranial magnetic stimulation: randomised multicentre trial. Br J Psychiatry. 191:441–448.
Hoshi E, Tanji J. 2004. Differential roles of neuronal activity in the supplementary and presupplementary motor areas: from information retrieval to motor planning and execution. J Neurophysiol. 92:3482–3499.
Hoshi E, Tanji J. 2007. Distinctions between dorsal and ventral premotor areas: anatomical connectivity and functional properties. Curr Opin Neurobiol. 17:234–242.
Hrabetova S, Sacktor TC. 1997. Long-term potentiation and long-term depression are induced through pharmacologically distinct NMDA receptors. Neurosci Lett. 226:107–110.
Huang YZ, Chen RS, Rothwell JC, Wen HY. 2007. The after-effect of human theta burst stimulation is NMDA receptor dependent. Clin Neurophysiol. 118:1028–1032.
Huang YZ, Edwards MJ, Rounis E, Bhatia KP, Rothwell JC. 2005. Theta burst stimulation of the human motor cortex. Neuron. 45:201–206.
Huang YZ, Rothwell JC, Lu CS, Wang J, Chen RS. 2010. Restoration of motor inhibition through an abnormal premotor-motor connection in dystonia. Mov Disord. 25:696–703.
Jakobs O, Langner R, Caspers S, Roski C, Cieslik EC, Zilles K, Laird AR, Fox PT, Eickhoff SB. 2012. Across-study and within-subject functional connectivity of a right temporo-parietal junction subregion involved in stimulus-context integration. Neuroimage. 60:2389–2398.
Jenkins IH, Jahanshahi M, Jueptner M, Passingham RE, Brooks DJ. 2000. Self-initiated versus externally triggered movements. II. The effect of movement predictability on regional cerebral blood flow. Brain. 123(Pt 6):1216–1228.
Kleim JA, Chan S, Pringle E, Schallert K, Procaccio V, Jimenez R, Cramer SC. 2006. BDNF val66met polymorphism is associated with modified experience-dependent plasticity in human motor cortex. Nat Neurosci. 9:735–737.
Koch G, Schneider S, Baumer T, Franca M, Munchau A, Cheeran B, Fernandez del Olmo M, Cordivari C, Rounis E, Caltagirone C et al. 2008. Altered dorsal premotor-motor interhemispheric pathway activity in focal arm dystonia. Mov Disord. 23:660–668.
Lemon RN. 2008. Descending pathways in motor control. Annu Rev Neurosci. 31:195–218.
Luppino G, Matelli M, Camarda R, Rizzolatti G. 1993. Corticocortical connections of area F3 (SMA-proper) and area F6 (pre-SMA) in the macaque monkey. J Comp Neurol. 338:114–140.
McAllister SM, Rothwell JC, Ridding MC. 2011. Cortical oscillatory activity and the induction of plasticity in the human motor cortex. Eur J Neurosci. 33:1916–1924.
McGuire PK, Bates JF, Goldman-Rakic PS. 1991. Interhemispheric integration: I. Symmetry and convergence of the corticocortical connections of the left and the right principal sulcus (PS) and the left and the right supplementary motor area (SMA) in the rhesus monkey. Cereb Cortex. 1:390–407.

Park JW, Kim YH, Jang SH, Chang WH, Park CH, Kim ST. 2010. Dynamic changes in the cortico-subcortical network during early motor learning. NeuroRehabilitation. 26:95–103.
Penny WD, Stephan KE, Mechelli A, Friston KJ. 2004. Comparing dynamic causal models. Neuroimage. 22:1157–1172.
Picard N, Strick PL. 2001. Imaging the premotor areas. Curr Opin Neurobiol. 11:663–672.
Prado J, Clavagnier S, Otzenberger H, Scheiber C, Kennedy H, Perenin MT. 2005. Two cortical systems for reaching in central and peripheral vision. Neuron. 48:849–858.
Quartarone A, Bagnato S, Rizzo V, Siebner HR, Dattola V, Scalfari A, Morgante F, Battaglia F, Romano M, Girlanda P. 2003. Abnormal associative plasticity of the human motor cortex in writer's cramp. Brain. 126:2586–2596.
Ragert P, Camus M, Vandermeeren Y, Dimyan MA, Cohen LG. 2009. Modulation of effects of intermittent theta burst stimulation applied over primary motor cortex (M1) by conditioning stimulation of the opposite M1. J Neurophysiol. 102:766–773.
Reetz K, Dogan I, Rolfs A, Binkofski F, Schulz JB, Laird AR, Fox PT, Eickhoff SB. 2012. Investigating function and connectivity of morphometric findings - Exemplified on cerebellar atrophy in spinocerebellar ataxia 17 (SCA17). Neuroimage. 62:1354–1366.
Rehme AK, Eickhoff SB, Wang LE, Fink GR, Grefkes C. 2011. Dynamic causal modeling of cortical activity from the acute to the chronic stage after stroke. Neuroimage. 55:1147–1158.
Ridding MC, Ziemann U. 2010. Determinants of the induction of cortical plasticity by non-invasive brain stimulation in healthy subjects. J Physiol. 588:2291–2304.
Rizzolatti G, Fogassi L, Gallese V. 2002. Motor and cognitive functions of the ventral premotor cortex. Curr Opin Neurobiol. 12:149–154.
Rizzolatti G, Luppino G. 2001. The cortical motor system. Neuron. 31:889–901.
Rizzolatti G, Luppino G, Matelli M. 1998. The organization of the cortical motor system: new concepts. Electroencephalogr Clin Neurophysiol. 106:283–296.
Rossini PM, Barker AT, Berardelli A, Caramia MD, Caruso G, Cracco RQ, Dimitrijevic MR, Hallett M, Katayama Y, Lucking CH. 1994. Non-invasive electrical and magnetic stimulation of the brain, spinal cord and roots: basic principles and procedures for routine clinical application. Report of an IFCN committee. Electroencephalogr Clin Neurophysiol. 91:79–92.
Rothwell JC, Hallett M, Berardelli A, Eisen A, Rossini P, Paulus W. 1999. Magnetic stimulation: motor evoked potentials. The International Federation of Clinical Neurophysiology. Electroencephalogr Clin Neurophysiol Suppl. 52:97–103.
Rouiller EM, Babalian A, Kazennikov O, Moret V, Yu XH, Wiesendanger M. 1994. Transcallosal connections of the distal forelimb representations of the primary and supplementary motor cortical areas in macaque monkeys. Exp Brain Res. 102:227–243.
Sarfeld AS, Diekhoff S, Wang LE, Liuzzi G, Uludag K, Eickhoff SB, Fink GR, Grefkes C. 2012. Convergence of human brain mapping tools: neuronavigated TMS parameters and fMRI activity in the hand motor area. Hum Brain Mapp. 33(5):1107–23.
Schubotz RI, von Cramon DY. 2003. Functional-anatomical concepts of human premotor cortex: evidence from fMRI and PET studies. Neuroimage. 20(Suppl 1):S120–S131.
Schuyler B, Ollinger JM, Oakes TR, Johnstone T, Davidson RJ. 2010. Dynamic causal modeling applied to fMRI data shows high reliability. Neuroimage. 49:603–611.
Shehzad Z, Kelly AM, Reiss PT, Gee DG, Gotimer K, Uddin LQ, Lee SH, Margulies DS, Roy AK, Biswal BB et al. 2009. The resting brain: unconstrained yet reliable. Cereb Cortex. 19:2209–2229.
Shimazu H, Maier MA, Cerri G, Kirkwood PA, Lemon RN. 2004. Macaque ventral premotor cortex exerts powerful facilitation of motor cortex outputs to upper limb motoneurons. J Neurosci. 24:1200–1211.
Stephan KE, Penny WD, Daunizeau J, Moran RJ, Friston KJ. 2009. Bayesian model selection for group studies. Neuroimage. 46:1004–1017.
Suppa A, Ortu E, Zafar N, Deriu F, Paulus W, Berardelli A, Rothwell JC. 2008. Theta burst stimulation induces after-effects on contralateral primary motor cortex excitability in humans. J Physiol. 586:4489–4500.
Talelli P, Cheeran BJ, Teo JT, Rothwell JC. 2007. Pattern-specific role of the current orientation used to deliver Theta Burst Stimulation. Clin Neurophysiol. 118:1815–1823.
Teo JT, Swayne OB, Rothwell JC. 2007. Further evidence for NMDA-dependence of the after-effects of human theta burst stimulation. Clin Neurophysiol. 118:1649–1651.
Terao Y, Ugawa Y. 2002. Basic mechanisms of TMS. J Clin Neurophysiol. 19:322–343.
Thickbroom GW. 2007. Transcranial magnetic stimulation and synaptic plasticity: experimental framework and human models. Exp Brain Res. 180:583–593.
Toni I, Krams M, Turner R, Passingham RE. 1998. The time course of changes during motor sequence learning: a whole-brain fMRI study. Neuroimage. 8:50–61.
Tsumoto T. 1992. Long-term potentiation and long-term depression in the neocortex. Prog Neurobiol. 39:209–228.
Van Dijk KR, Hedden T, Venkataraman A, Evans KC, Lazar SW, Buckner RL. 2010. Intrinsic functional connectivity as a tool for human connectomics: theory, properties, and optimization. J Neurophysiol. 103:297–321.
Wang LE, Fink GR, Diekhoff S, Rehme AK, Eickhoff SB, Grefkes C. 2011. Noradrenergic enhancement improves motor network connectivity in stroke patients. Ann Neurol. 69:375–388.
Ward NS, Brown MM, Thompson AJ, Frackowiak RS. 2003. Neural correlates of motor recovery after stroke: a longitudinal fMRI study. Brain. 126:2476–2496.
Yousry TA, Schmid UD, Alkadhi H, Schmidt D, Peraud A, Buettner A, Winkler P. 1997. Localization of the motor hand area to a knob on the precentral gyrus. A new landmark. Brain. 120(Pt 1): 141–157.
Zafar N, Paulus W, Sommer M. 2008. Comparative assessment of best conventional with best theta burst repetitive transcranial magnetic stimulation protocols on human motor cortex excitability. Clin Neurophysiol. 119:1393–1399.
Ziemann U, Lonnecker S, Steinhoff BJ, Paulus W. 1996. The effect of lorazepam on the motor cortical excitability in man. Exp Brain Res. 109:127–135.
zu Eulenburg P, Caspers S, Roski C, Eickhoff SB. 2012. Meta-analytical definition and functional connectivity of the human vestibular cortex. Neuroimage. 60:162–169.